

**NUMERICAL MODELING AND SIMULATION OF A MASONRY  
ARCH IN ANSYS SUBJECTED TO IMPACT LOADING**

**Sajjad Ahmad, Giuseppe Andrea Ferro, Abdul Qadir Bhatti,  
Rao Arsalan Khushnood and Aitizaz Arshad**



# NUMERICAL MODELING AND SIMULATION OF A MASONRY ARCH IN ANSYS SUBJECTED TO IMPACT LOADING

By

**Sajjad Ahmad, Giuseppe Andrea Ferro, Abdul Qadir Bhatti, Rao Arsalan  
Khushnood, Aitizaz Arshad**

## Abstract

The present research work describes the numerical modeling of the masonry arch structures under the impact loadings. The performance of the numerical model for impact loading was compared with the laboratory test results. Several finite element models with different level of complexities and assumptions were generated and subsequently analyzed in ANSYS. The finite element models were tested for linear static, dynamic and impact loadings. The results produced by the finite element models showed upper bound results for the arch structure. This investigation will help in understanding the performance of masonry arch bridges in mountainous regions vulnerable to seismic loadings and falling rocks impact. The performance assessment will also help in performing rehabilitation and restoration of the historical structures and monuments. The finite element modeling (FEM) is a much diversified technique. Its utilization in modeling saves lot of efforts and cost in analyzing the behaviors of the materials and structures subjected to any kind of loading conditions. In present case the material models were calibrated to suit the performance of the tested structures. The finite element models were then validated with the impact performance of the laboratory tested masonry arches.

**Key words:** Finite element analysis; FEM, Impact load; Masonry; Arch; ANSYS; Numerical analysis; Falling weight impact test

## 1. Introduction

Stone and masonry arch structures have been serving the humanity since ancient times. Still today they form a significant portion of the transportation infrastructure. In hilly regions road and railway bridges are generally constructed from masonry or stone arches due to the easy availability of the construction material (stone, masonry etc.). In addition to normal loadings these bridge structures have to withstand the extreme loading conditions offered by the natural as well as man-made hazards such as earthquakes, land slidings, debris flows, falling rocks fast moving projectiles, blasts and shock waves from explosions (Milani, et al., 2012). In those regions due to high seismicity levels and sharp slopes land slidings and rocks falling are common, causing high impact loadings on the bridge structures. So it is necessary to rehabilitate and upgrade the existing facilities or construct new facilities/structures that are capable of sustaining such loadings and remain in service.

## 2. Research significance

The performance analysis of masonry arch structures under the impact loading leads to the better understanding of the phenomenon. This helps in the development of the resistance curve of the structural system that can be further utilized for similar structures. The present research discusses the significant parameters involved in the accurate numerical modeling of the masonry structures and also the best suited numerical techniques.

### 3. Impact load mechanism

The impact load is defined as a high force or shock applied to an object in a very short time period; such as the collision of the two or more relatively moving bodies. The magnitude of the impact force generated by the collision is much greater as compared to the load applied statically (Alves, et al., 2006). The mechanism of the impact force is based on the principal of energy conservation. The moving body/object transfers its momentum energy in to the striking object. The transferred energy is partially converted in to the strain energy in the target and partially dissipates in terms of friction, heat and sound energies. The impact force depends upon the deformability of the striking object and the laws of mechanics show that the assumption of the rigid body is not valid in this case as that will result in zero deformation thus leading to the infinite force. In civil engineering structures the deceleration, momentum transfer and deformations are dictated by the elastic and plastic behavior of the construction materials. So it is important to do rational estimates of the local stiffness and the corresponding deformation at the points of impacts (Cancelliere, et al., 2010).

### 4. Materials

The arch constructed for laboratory impact testing was made up of granite stone blocks. Granite is a strong rock and has been used in the construction of many ancient building and structures. The visual inspection indicated that granite blocks have fine to medium grained structure. The average density and porosity of the stone blocks is given in table 1.

Table-1: Physical properties of stone blocks

Granite type	Porosity (%)	Density (kg/m <sup>3</sup> )	
		Dry	Saturated
Fresh granite	0.47	2660	2665
Weathered granite	3.56	2579	2614

The mechanical properties were determined and it was found that the granite stone was strong in compression and showed brittle type of failure. The flexural strength came out to be very low as compared to the compression strength of the rock. Typical stress strain curve is shown below.

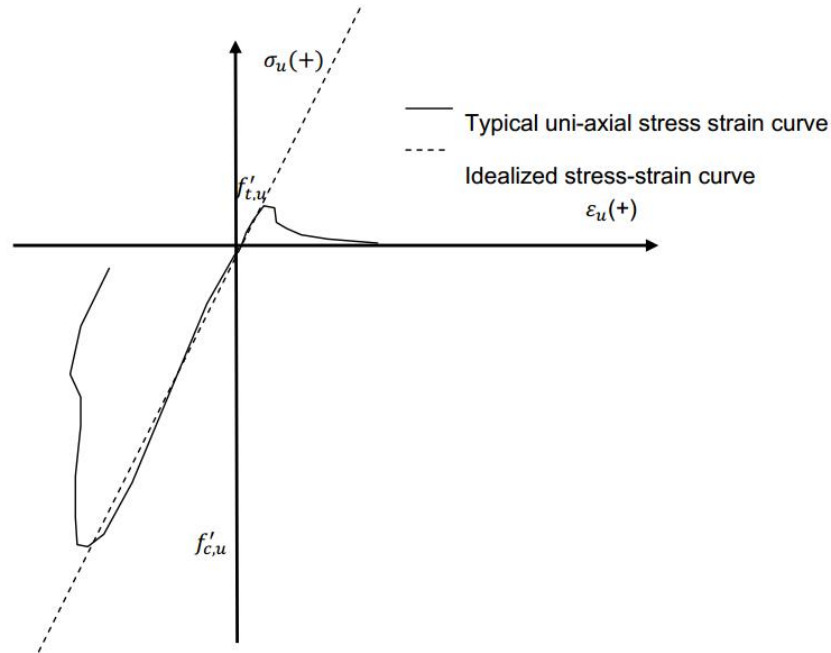


Figure 1: Typical uni-axial stress strain behavior of granite

The average compressive and flexure strengths of the granite are shown in table 2. Lime mortar was used to join the masonry blocks. Small samples of the lime mortars were made and tested only for compressive strength. The outcome of the strength tests of lime mortar are also given in table below.

Table 2: Mechanical properties of materials used

		<b>Fresh granite</b>	<b>Weathered granite</b>
<b>Compression</b>	Elastic modulus GPa	52.25	35.09
	Peak compressive strength MPa	148.00	90.00
	Poisson's ratio	0.23	0.30
<b>Tension</b>	Elastic modulus GPa	12.55	3.18
	Peak tensile strength Mpa	6.01	3.52
	Fracture energy MPa	0.148	0.200
		Lime mortar	
<b>Compression</b>	Elastic modulus MPa	200.00	
	Peak compressive strength MPa	22.00	
	Poisson's ratio	0.10	

## 5. Experimental setup

The segmental type stone masonry arch constructed for impact testing was made up of 13 identical stone blocks. The blocks were joined with the lime mortar. The clear span was kept about 1.2 m (47.24 in). The clear height of the model arch was limited to 0.4 m (15.75 in). The radial thickness of the stone blocks was fixed as 0.16 m (6.30 in). A steel ball of 60.9 kg was used to provide the impact force by falling through a distance of 0.70 m (27.55 in) height above the point of impact. The impact load was applied at the quarter of the span (i.e. 0.4 m or 15.75 in from left of the support). The experimental setup was equipped with load cells and LVDTs for measuring and recording the displacements under the point of impact and crown of the arch. The experimental setup is shown below in figure 2. The impact load and time histories were also recorded by using load cells. The smoothing treatment was applied to the recorded data to eliminate the noise from the recorded data. After that treatment the experimental data was compared with the numerical results obtained from finite element simulations.

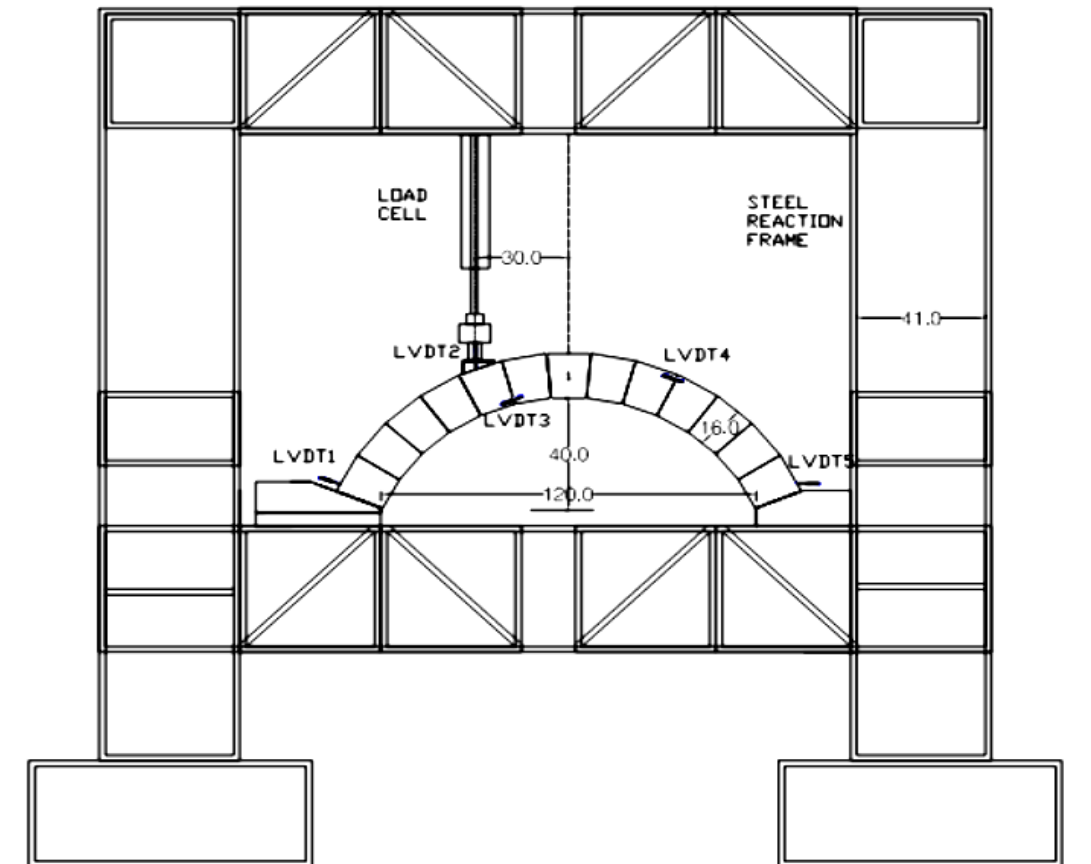


Figure 2: Experimental setup of stone masonry arch

## 6. Numerical model

The arch was modeled in ANSYS v14.0 which is explicit type of finite element software. For better understanding of the impact behavior on different configuration of arches three types of FE models were developed. a) Arch with stone blocks having smooth dry

joints, b) arch with stone blocks having rough dry joints and c) arch with rough ended stone blocks having wet joints or lime mortar joints (Ghiassi, et al., 2012).



Figure 3: Smooth dry joints

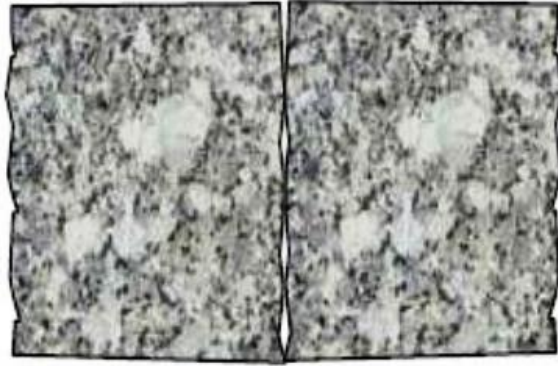


Figure 4: Rough dry joints

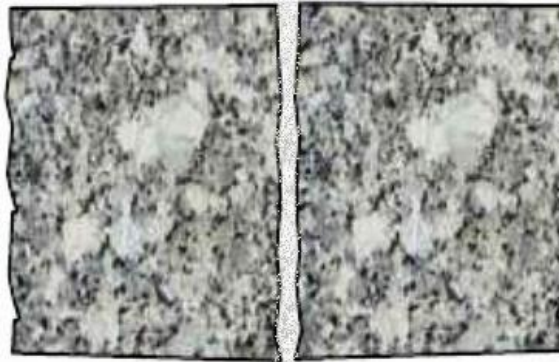


Figure 5: Rough wet joints

The physical and mechanical properties of the materials used in the construction and modeling of arch are mentioned above in table 1 and 2. The mechanical properties of the materials were investigated under static loading. The literature suggests that a Dynamic Increase Factor (DIF) should be incorporated if the applied loading on the structure is not static such as impact etc. The materials exhibit higher mechanical strength if the strain rate or rate of loading is higher (Gilbert, et al., 2002). The CEB model code recommends that the DIF is governed by following equations:

$$DIF = \frac{\hat{f}'_c}{f'_c} = \left( \frac{\dot{\epsilon}_d}{\dot{\epsilon}_o} \right)^{1.026\alpha} \quad \text{for } |\dot{\epsilon}_d| \leq 30 \text{ s}^{-1}$$

$$DIF = \frac{\hat{f}'_c}{f'_c} = \gamma_s \left( \frac{\dot{\epsilon}_d}{\dot{\epsilon}_o} \right)^{1/3} \quad \text{for } |\dot{\epsilon}_d| > 30 \text{ s}^{-1}$$

$$\alpha = \frac{1}{5 + 9 \frac{f'_c}{f'_o}} \quad \text{and} \quad \log \gamma_s = 6.156\alpha - 2$$

Where as

Here  $f'_c$  is the quasi static unconfined compressive strength,  $\hat{f}'_c$  is the dynamic unconfined compressive strength,  $\dot{\epsilon}_d$  is the strain rate and  $f'_o$ ,  $\dot{\epsilon}_o$  are the constants having the

values of 10MPa and  $30 \times 10^{-6} \text{ s}^{-1}$ . CEB model fitting curve show that for impact loading cases the DIF varies from 1.4 to 3.1(Schwer, 2009).

The FE model of the arch was developed in ANSYS by using plane stress elements. The default rigid supports were considered for the arch in the ANSYS model. The model is shown in figure 5. The impactor was modeled as spherical steel ball with the diameter calculated by considering mass of impactor and the steel density. The velocity of the steel ball at the point of impact was based on the height of fall of the impactor. For validation of the arch model mesh dependency was investigated. In this technique the mesh size of the model is varied while keeping all other conditions constant such as loading and boundary conditions. The geometric model that exhibits constant stresses and displacements with respect to various mesh sizes is considered accurate(Lourenço, et al., 2012). Mesh independency of the model was analyzed for its self-weight. The maximum deflections and the maximum stresses were recorded for each size and compared afterwards. The model results indicate similar level of stresses and deflection in the model i.e. mid span deflection of 0.682 mm with corresponding von misses stress of 841 Pa. This indicates that the geometrical model of the arch is valid and without any flaw.

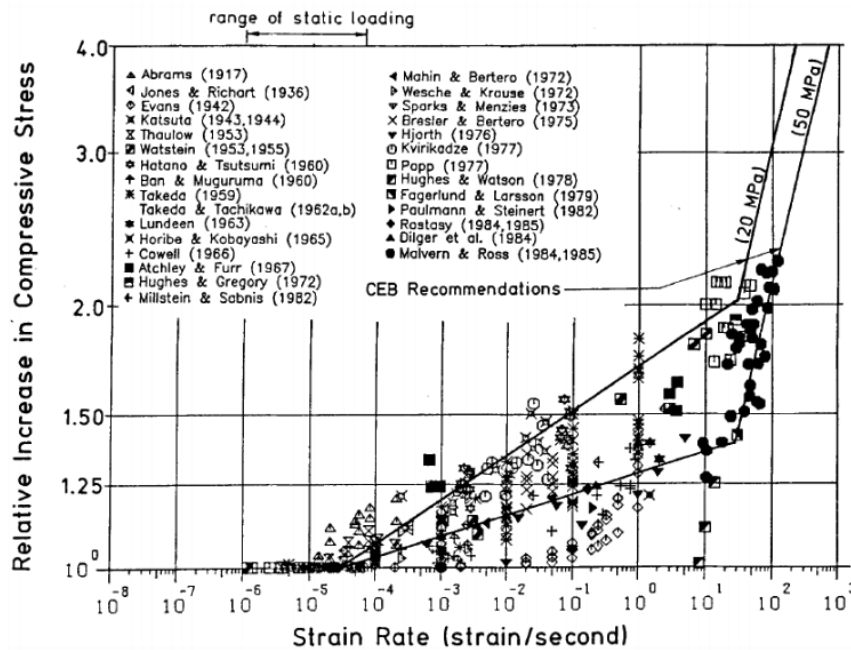


Figure 6: Log-log scale strength increase factor verses strain rate



Figure 7: Geometry of arch model

The validated geometric model was further analyzed for four impact load cases by varying the impactor mass and height of fall. The detail of the load cases is given below:

Table 2: Load cases for finite element model analysis

Nomenclature	Height of fall (m)	Mass of impactor (kg)	Impact velocity (m/s)	Energy at the point of impact (J)
M60H70Q	0.70	60.90	3.71	419.11
M80H45Q	0.45	80.00	2.97	357.57
M60H70M	0.70	60.90	3.71	419.11
M80H45M	0.45	80.00	2.97	357.57

Two sets of impact positions were investigated namely quarter and mid span indicated by 'Q' and 'M' respectively in the naming convention.

## 7. Comparison of FE model results and experimental results

The laboratory test results of arch 'M60H70Q' were compared with the numerical simulation results. The tested arch showed the formation of two hinges, one rotation and one sliding hinge at left support and right support respectively. The FE model also depicted the same phenomena as indicated in the figure below:

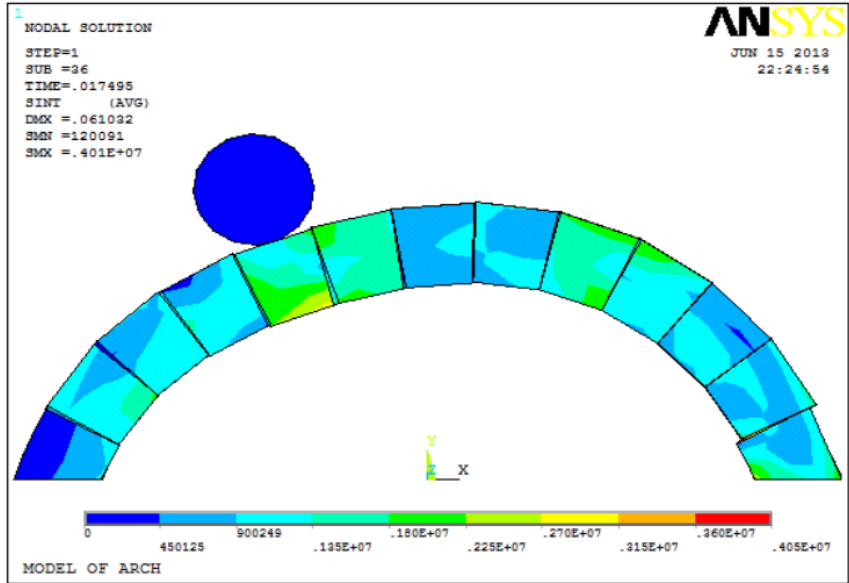


Figure 8: Stress variation and hinge formation in the FE model

The maximum deflection were compared for experimental and FE model results. The numerical model gives about 15.62% lesser deflection as compared to the experimental results. This indicates that the numerical model is capable to provide a good estimate of the deflections in the arch.

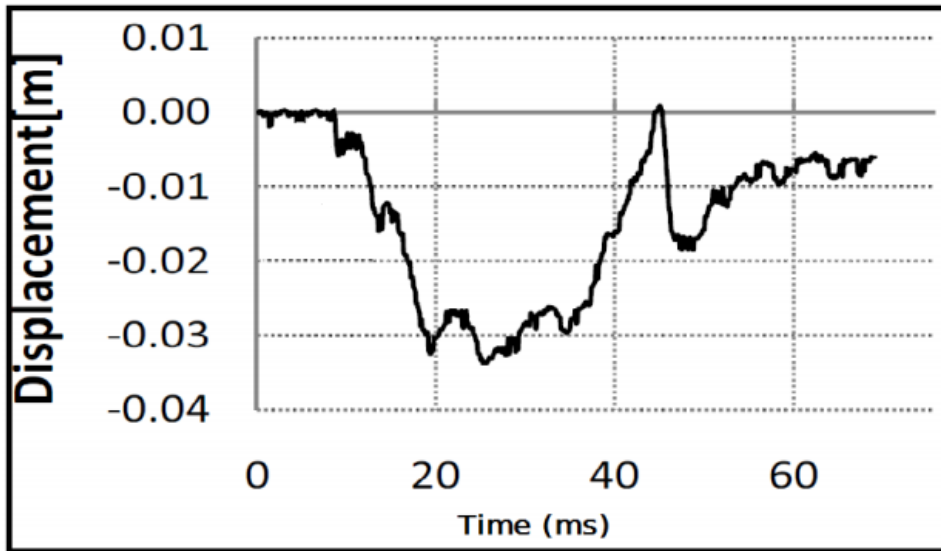


Figure 9: Time history of deflection in experimental arch

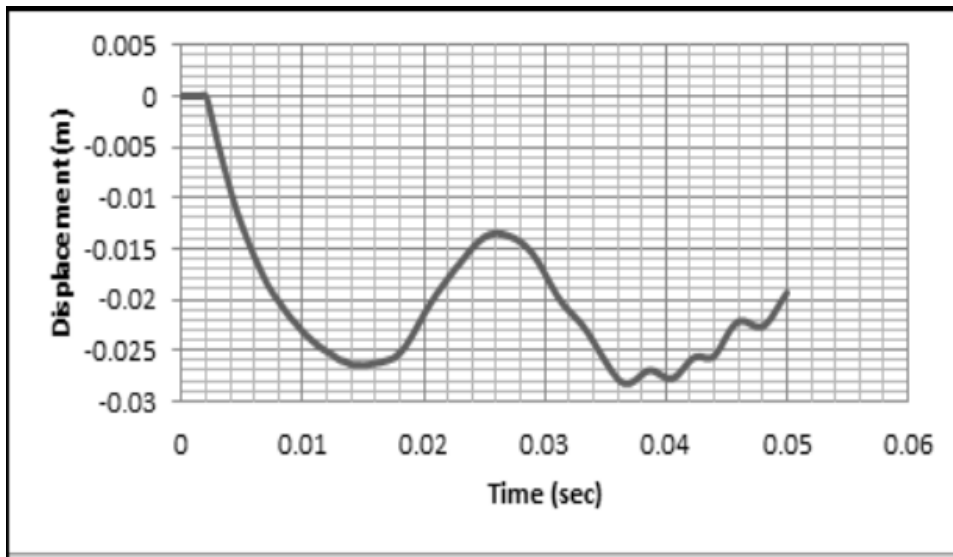


Figure 10: Time history of deflection by numerical model of the arch

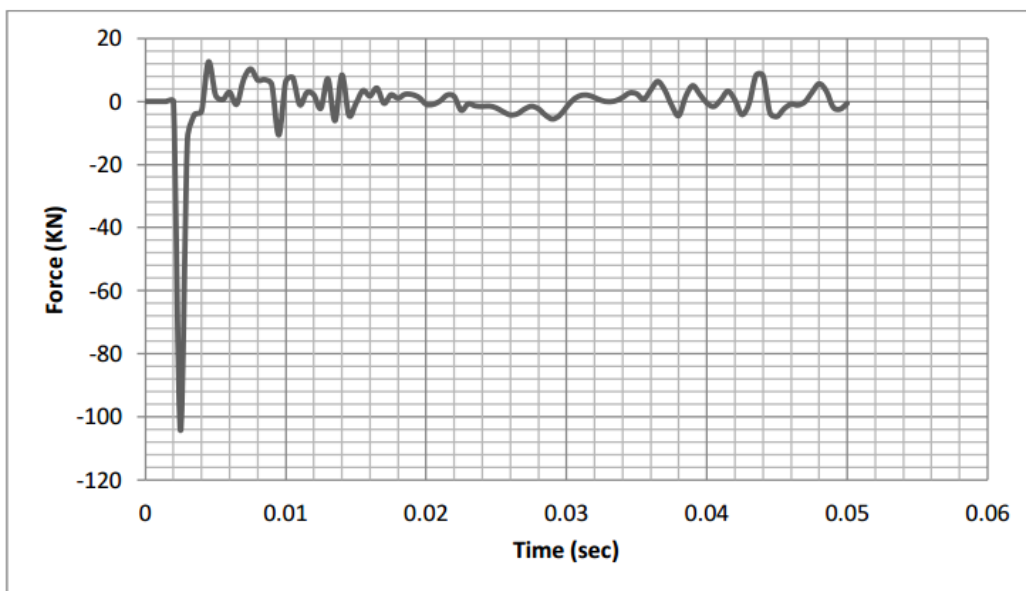


Figure 11: Impact force for 'M60H70Q' at quarter span

The impact force increases with the increase in fall height or mass of the impactor. The impact force was observed relatively larger at the mid span as in this case all the kinetic energy contributes towards the impact force whereas for quarter span application some kinetic energy is utilized in pushing the arch side way hence reducing the vertical impact force a little bit.

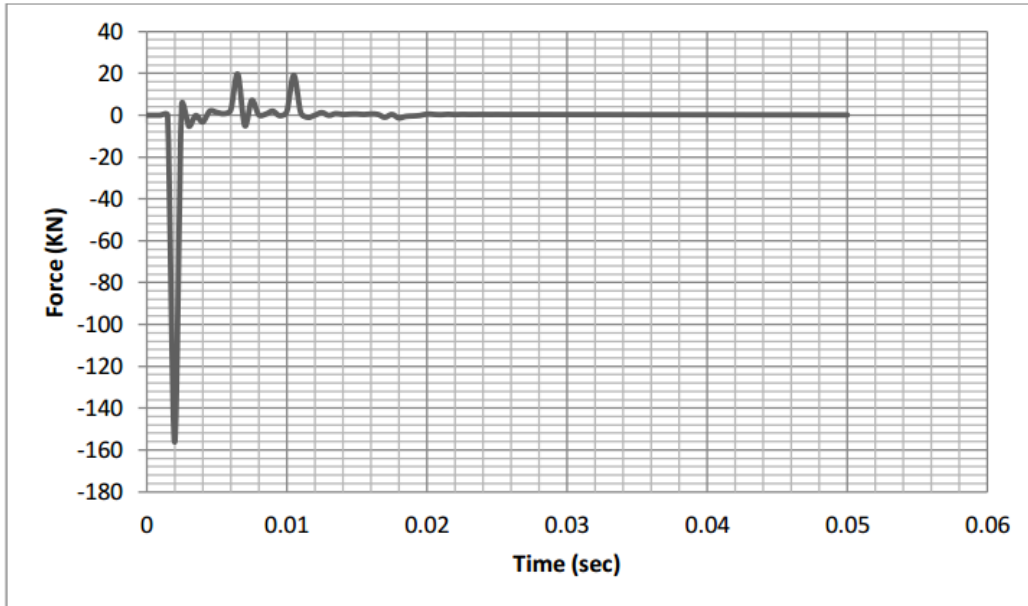


Figure 12: Impact force for 'M80H75Q' at quarter span

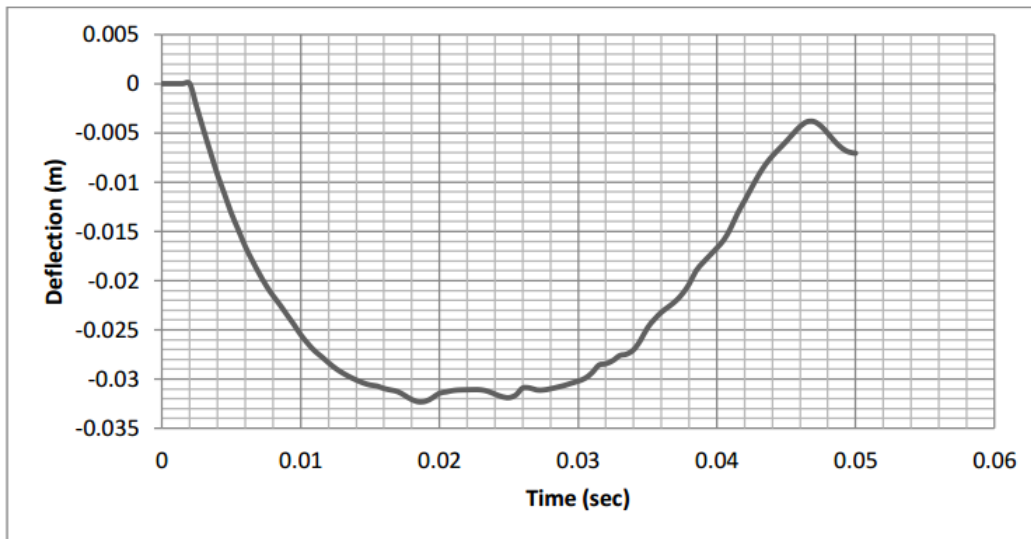


Figure 13: Mid span deflection for 'M60H70M'

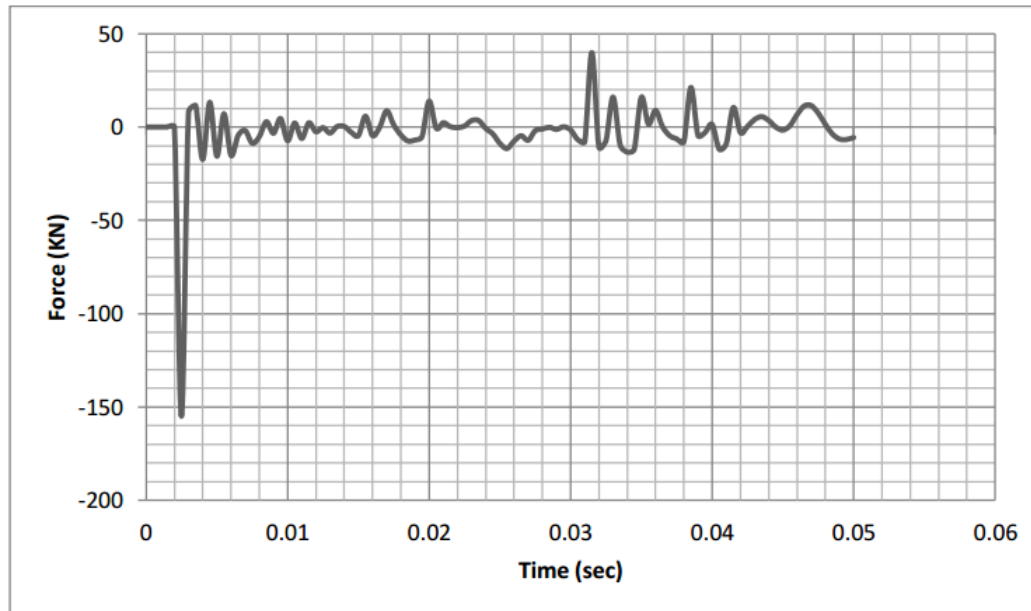


Figure 14: Impact force for 'M60H70M' at mid span

## 8. Conclusions

In the present research work a numerical model of an arch was developed in ANSYS and it was compared with the experimental results. The results indicate that the finite element models can help in assessing the performance of the stone masonry arches under impact loading due to falling weights. An error of about 15% was observed but it may be negotiated on considering more sophisticated modeling of the structure and load application techniques. The improved numerical models may accurately depict the performance of the structure making them safer to design as well as saving the cost and time that is required for mechanical testing.

## Bibliography

- Alves Marcilio e Oshiro Roberto Eiki** Scaling the impact of a mass on a structure [Rivista] // International Journal of Impact Engineering. - 2006. - Vol. 32. - p. 1158-1173.
- Beygi B Shieh** Numerical analysis of structural masonry: mesoscale approach [Rivista] // Computers and Structures. - 2008. - Vol. 86. - p. 1958-1973.
- Cancelliere Ilaria, Imbimbo Maura e Sacco Elio** Experimental tests and numerical modeling of reinforced masonry arches [Rivista] // Engineering Structures. - 2010. - Vol. 32. - p. 776-792.
- De Luca Antonello, Giordano Aldo e Mele Elena** A simplified procedure for assessing the seismic capacity of masonry arches [Rivista] // Engineering Structures. - 2004. - Vol. 26. - p. 1915-1929.
- Dejong Matthew J** Seismic response of stone masonry spires: Analytical modeling [Rivista]. - 2012. - Vol. 40. - p. 556-565.
- Ghiassi Bahman [et al.]** Numerical analysis of bond behavior between masonry bricks and composite materials [Rivista] // Engineering Structures. - 2012. - Vol. 43. - p. 210-220.

- Gilbert M, Hobbs B e Molyneaux T. C. K** The performance of unreinforced masonry walls subjected to low velocity impacts: mechanism analysis [Rivista] // International Journal of Impact Engineering. - 2002. - Vol. 27. - p. 253-275.
- Grande Ernesto, Imbimbo Maura e Sacco Elio** Modeling and numerical analysis of the bond behavior of masonry elements strengthened with SRP/SRG [Rivista] // Composites: Part B. - 2013. - Vol. 55. - p. 128-138.
- Lourenço Paulo B [et al.]** Seismic performance of the St. George of the Latins church: Lessons learned from studying masonry ruins [Rivista] // Engineering Structures. - 2012. - Vol. 40. - p. 501-518.
- Milani Gabriele e Lourenco Paulo B** 3D non linear behavior of masonry arche bridges [Rivista] // Computers and Structures. - 2012. - Vol. 110-111. - p. 133-150.
- Nazir Shahid e Dhanasekar Manicka** Modelling the failure of thin layered mortar joints in masonry [Rivista] // Engineering Structures. - 2013. - Vol. 49. - p. 615-627.
- Pérez-Aparicio J L, Bravo R e Ortiz P** Refined element discontinuous numerical analysis of dry contact masonry arches [Rivista] // Engineering Structures. - 2013. - Vol. 48. - p. 578-587.
- Schwer Leonard E** Strain rate induced strength enhancement in concrete: much ado about nothing [Atti di convegno] // 7th European LS-DYNA Conference. - 2009.
- Smoljanovic Hrvoje, Zivaljic Nikolina e Nikolic Zeljana** A combined finite discrete element analysis of dry stone masonry structures [Rivista] // Engineering Structures. - 2013. - Vol. 52. - p. 89-100.
- Wang S Y [et al.]** Numerical simulation of the failure mechanism of circular tunnels in transversely isotropic rock masses [Rivista] // Tunnelling and Underground Space Technology. - 2012. - Vol. 32. - p. 231-244.